The XPS, depth profile analysis and photoluminescence studies of pulsed laser deposited $SrAl_2O_4:Eu^{2+}$, Dy^{3+} thin films prepared using different laser fluencies

P.D. Nsimama[1], O.M. Ntwaeaborwa[2] and H.C Swart[2]

[1] Department of Science and Laboratory Technology, Dar Es Salaam Institute of Technology, P.O. Box 2958, Dar Es Salaam, Tanzania.

[2]Physics Department, University of the Free State, P. O. Box 9300, Bloemfontein, South Africa.

Corresponding author; pnsimama@yahoo.com

Abstract

$SrAl_2O_4:Eu^{2+}$, Dy^{3+} thin films were grown on silicon (Si) (111) substrates using the pulsed laser deposition (PLD) technique to investigate the influence of the laser fluence on the structure, morphology and photoluminescent properties of the films. The atomic force microscopy (AFM), scanning electron microscopy (SEM), X-ray Diffraction (XRD), energy dispersive x-ray spectroscopy (EDS), photoluminescence (PL) spectroscopy and the x-ray photoelectron spectroscopy (XPS) were used to characterize the films. The $SrAl_2O_4:Eu^{2+}$, Dy^{3+} thin films gave two green PL emissions peaks coming from Eu^{2+} ions occupying the two Sr^{2+} sites in the $SrAl_2O_4$ host lattice. The green emissions were attributed to $4f^65d^1 \rightarrow 4f^7$ transitions of Eu^{2+}. The films with well-defined grains gave superior PL intensity and long afterglow characteristics. The EDS and XPS results showed that the films consisted of all the major elements (i.e. Sr, Al and O) present in $SrAl_2O_4:Eu^{2+}$, Dy^{3+} material. The carbon (C) and the Si peak from the substrate were also identified. The XPS depth profile results showed a linear relationship of the film thickness with the laser fluence. The variations of surface morphological and topographical properties of the films with the laser fluencies are discussed.

Keywords: $SrAl_2O_4:Eu^{2+}$,Dy^{3+}, PL, thin film, laser fluence, XPS

1. Introduction

There has been an increase in the reports on $SrAl_2O_4:Eu^{2+}$, Dy^{3+} phosphor in the past few years due to its potential application in infrastructure. This follows from the fact that the material can glow for more than 50 hours after cutting off the excitation source [1]. The afterglow property of $SrAl_2O_4:Eu^{2+}$, Dy^{3+} makes it a potential candidate for luminous paints in highway poles, glowing house numbers, rural lighting, etc. For industrial applications, thin films are preferred because of better thermal stability, less out gassing and better adhesion to the solid substrate. Among the popular thin-film preparation techniques, the pulsed laser deposition (PLD) technique has become increasingly important because of its use of small target materials, high deposition rate and capability stoichiometric transfer [2]. The control of the $SrAl_2O_4:Eu^{2+}$, Dy^{3+} film properties using the PLD deposition parameters have been reported elsewhere [3-7]. Ntwaeaborwa et al. [3] and Sato et al. [4] reported that brighter green emissions were coming from $SrAl_2O_4:Eu^{2+}$, Dy^{3+} films deposited on a 350-400^o C substrate temperature range. It was also noted [3] that $SrAl_2O_4:Eu^{2+}$, Dy^{3+} films deposited using higher number of pulses gave better PL and afterglow properties. Nsimama et al. [5] reported that $SrAl_2O_4:Eu^{2+}$, Dy^{3+} thin films deposited in the argon and oxygen gas atmospheres had AFM images with well-defined grains, superior PL emission intensity and long lifetimes compared to the films prepared in vacuum.

More investigations on the influence of PLD deposition parameters on the PL properties of pulsed laser deposited $SrAl_2O_4:Eu^{2+}$, Dy^{3+} thin films need to be done in order to optimize luminescent properties of $SrAl_2O_4:Eu^{2+}$, Dy^{3+}. The laser fluence is one of the critical deposition parameters in PLD experiments. This is due to the fact that, the energy absorbed in the target material per unit surface area depends on the laser fluence implying that the ablation rate is a function of fluence [8]. The primary objective

of this study was therefore to investigate the influence of the laser fluence on the surface states and PL properties of $SrAl_2O_4:Eu^{2+}$, Dy^{3+} films prepared by the PLD technique. The elemental composition analysis was done by using the X-ray photoelectron spectroscopy (XPS).

2. Experimental details

Pellets for ablation were prepared from a commercial $SrAl_2O_4:Eu^{2+}$, Dy^{3+} powder phosphor from Phosphor Technology in the United Kingdom. The deposition chamber was evacuated to a base pressure of 8×10^{-6} mbar. The Lambda Physic 248 nm KrF excimer laser was used to ablate the phosphor pellet in the oxygen atmospheres. The laser fluence was varied during depositions while other deposition conditions were kept constant. The oxygen pressure (purity 99.999 %), substrate temperature, and the substrate-distance were fixed at 348 mTorr, 400° C and 6 cm respectively. The films were deposited on Si (111) substrate with an area of 1 cm^2. The Shimadzu Superscan SSX-550 system was used to record the SEM and EDX data. AFM pictures were obtained from the Shimadzu SPM - 9600 model. The SIEMENS D5000 diffractometer using Cu Kα radiation of λ = 1.5405 nm was used for XRD data collection. The PL data were collected by the PL system using the 325 nm He-Cd laser as the excitation source, and the decay curves were recorded from the Cary Eclipse fluorescence spectrophotometer using monochromatic xenon lamp as excitation source. The XPS data were obtained by using a PHI 5000 Versa probe – Scanning ESCA Microprobe. The XPS surveys were done with a 100 μm 25 W 15 kV Al monochromatic x-ray beam and the depth profiling analyses were done with a 2 kV 2 μA 2x2 mm raster – Ar ion gun. The sputter rate was 8.5 nm/min.

3. Results and Discussion

3.1 SEM Results

Figure 1 shows the SEM images of $SrAl_2O_4:Eu^{2+},Dy^{3+}$ thin films deposited at different laser fluencies. The film deposited at the lowest laser fluence of 1.03 J/cm^2 (Fig.1 (a)) has a surface consisting of microcracked feature with several spherical droplets formed from agglomeration of phosphor grains. The film deposited at laser fluence 1.27 J/cm^2 consists of a relatively smoother layer and few phosphor grains of spherical and irregular shapes. The surface of the film deposited at 1.78 J/cm^2 laser fluence consists of spherical grains covering the entire area. The microcracks for this sample are most pronounced, the result that is attributed to the higher temperature of the deposited particles at higher laser fluence [9].

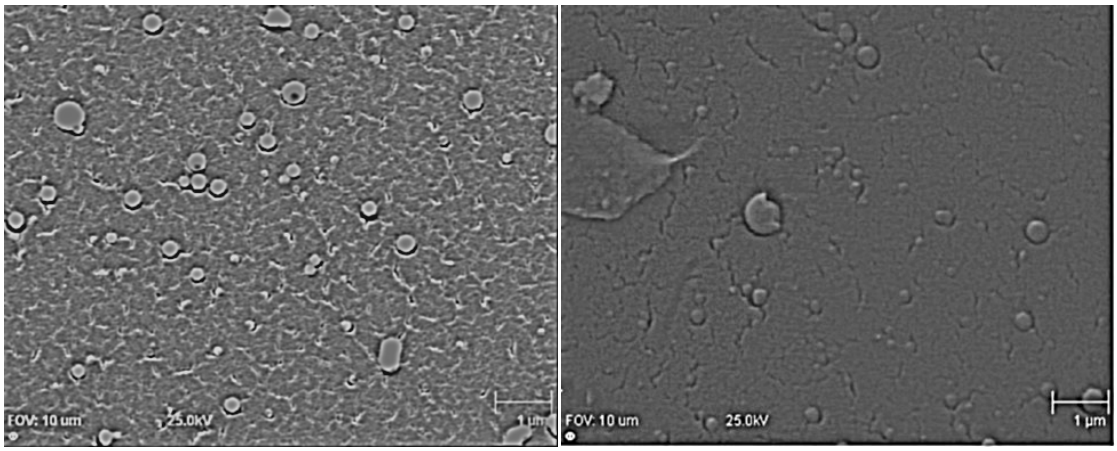

(a) (b)

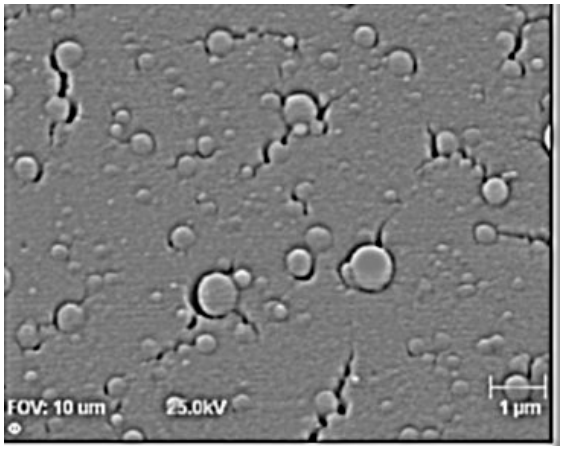

(c)

Fig. 1. The SEM images for thin films deposited at different laser fluencies; (a) 1.03 J/cm², (b) 1.27 J/cm² and (c) 1.78 J/cm²

The EDS elemental compositions for the films deposited at different laser fluencies are shown in Figure 2. The films display EDS spectra consisting of all the main elements of $SrAl_2O_4:Eu^{2+}Dy^{3+}$, (the host material) i.e. Sr, Al, and O. The Si substrate and adventitious C were also detected. In all the spectra, Sr peaks were embedded on the Si peaks. The intensities of O and Al were varying proportionally with the laser fluencies and inversely proportional with the Si. It can be observed from the results that the sample deposited at the highest laser fluence gave the highest intensity of O and Al and lowest value of Si, due to the substantial film thickness resulting from the high laser fluence. The results suggest that, the films deposited at higher fluencies have lower contents of Si and C and higher contents of Al, O and Sr.

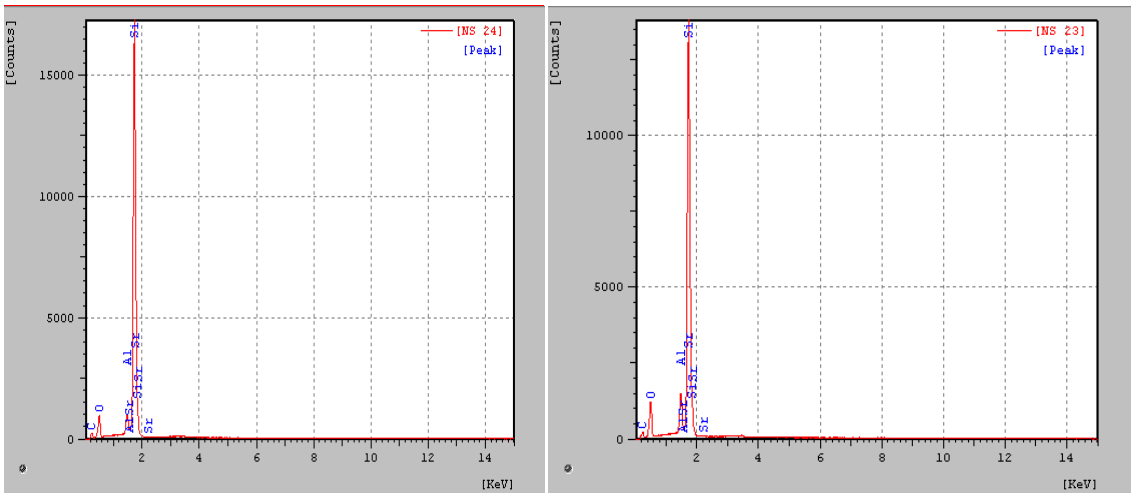

(a) (b)

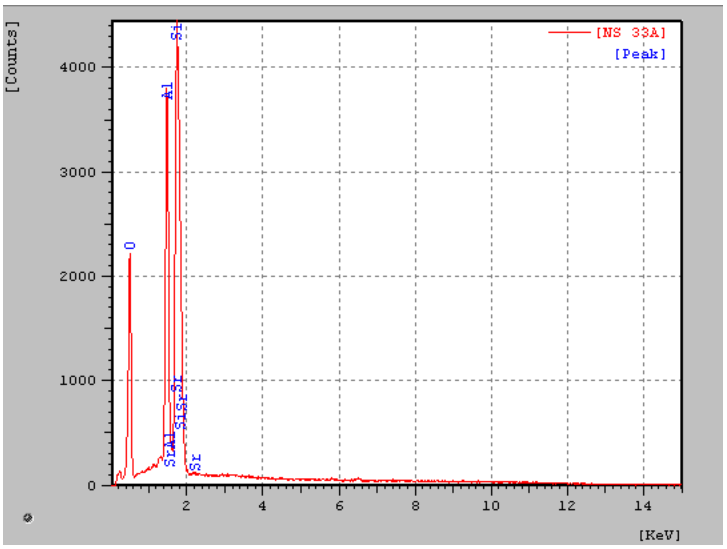

(c)

Fig. 2. EDS spectra for PLD $SrAl_2O_4:Eu^{2+}$, Dy^{3+} thin films deposited at different laser fluencies; (a) 1.03 J/cm² (b) 1.27 J/cm², (c) 1.78 J/cm².

3.2 AFM Results

The AFM images of $SrAl_2O_4:E^{u+},Dy^{3+}$ thin films deposited at different laser fluences are shown in Figure 3. The surface of the film deposited at 1.03 J/cm² was characterized by poorly-defined grains and agglomeration of nanoparticles. Well-defined grains are observed on the surface of the AFM image of the film deposited at 1.27 J/cm² laser fluence. The surface of the film deposited at highest fluence is characterized by particles agglomeration forming big vertical clusters. The particles in this case seem to be bigger

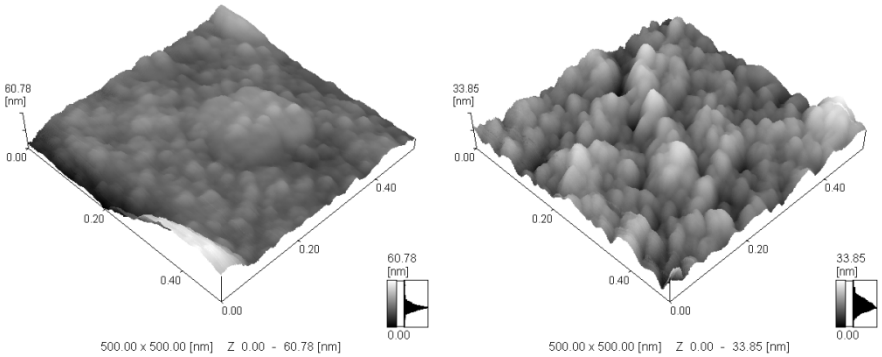

(a) (b)

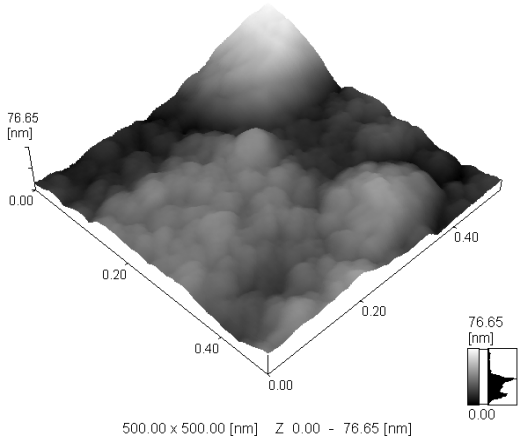

(c)

Fig. 3. The AFM images of $SrAl_2O_4:E^{u+},Dy^{3+}$ thin films ablated at different laser fluencies; (a) 1.03 J/cm² (b) 1.27 J/cm², (c) 1.78 J/cm²

than in the other two samples and the shadows observed are resulting from erected agglomerated nanoparticles. It can be deduced from the AFM results that, films with well-defined grains favour the intermediate values of laser fluencies. The next sections discusses the structure and PL properties of the three films.

3.3 XRD Results

The XRD results for our as-deposited thin films were all amorphous (not shown). Amorphous structures for the as-deposited $SrAl_2O_4:Eu^{2+}$, Dy^{3+} thin films have also been reported in previous works [3-5, 7].

3.4 Photoluminescence (PL) Results

The room temperature PL results for the $SrAl_2O_4:Eu^{2+},Dy^{3+}$ films deposited at different laser fluencies are shown in Figure 4. All the films give green emission with varying intensities. Films deposited at lower laser fluencies (1.03 and 1.27 J/cm²) give green emission peaks at two different positions coming from two different crystallographic positions of Eu^2in $SrAl_2O_4:Eu^{2+},Dy^{3+}$ material [10]. The film deposited at 1.78 J/cm² have only one green peak, suggesting that at higher laser fluencies only one Sr^{2+} site is actively involved in the $SrAl_2O_4:E^{2+},Dy^{3+}$ green emission process. The PL shoulder at around 621 nm recorded by this sample is possibly coming from unreduced Eu^{3+} during the powder preparation process as reported elsewhere [11]. It is also worth noting that there is a red-shift of the main green peak position for the sample deposited at highest laser fluence, attributed to the increased particle sizes. The highest green emission intensity is recorded by the film deposited at 1.27 J/cm² laser fluence.

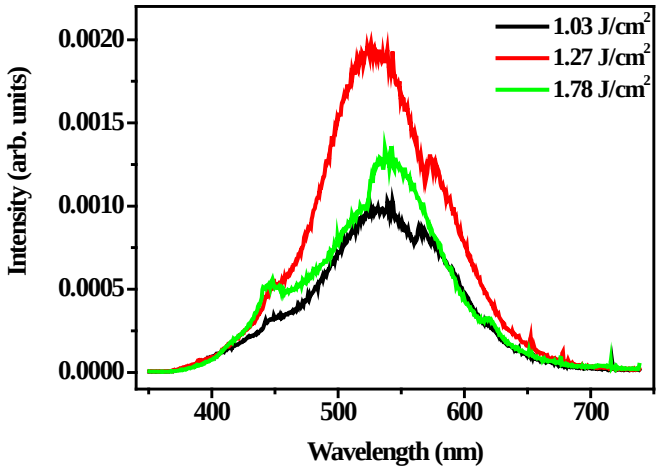

Fig. 4. The room temperature photoluminescence spectra of $SrAl_2O_4:Eu^{+},Dy^{3+}$ thin films deposited at different laser fluencies.

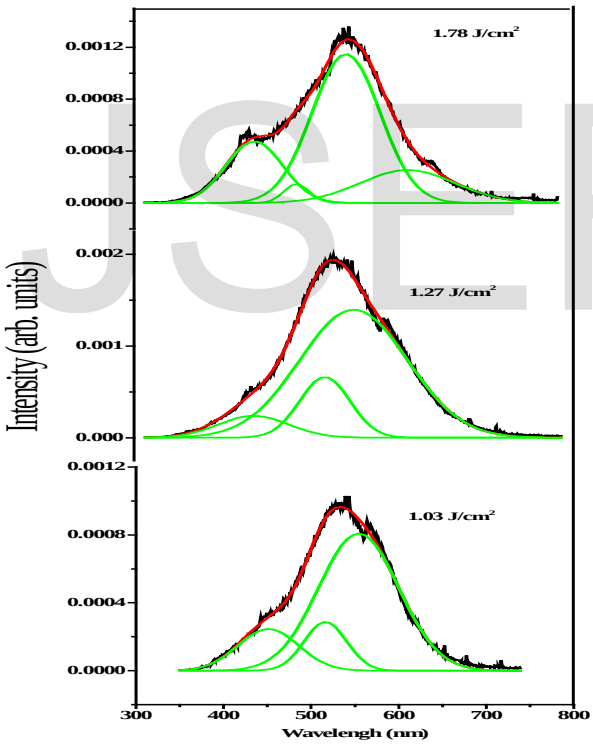

Fig. 5. The deconvoluted Gaussian peaks for $SrAl_2O_4:Eu^{2+},Dy^{3+}$ thin films deposited at different laser fluencies.

The green and red emissions comes from the $4f^65d^1 \rightarrow 4f^7$ and $^5D_0 \rightarrow {}^7D_2$ transitions of Eu^{2+} and Eu^{3+} [5] respectively. It can also be observed that all the films have shoulders on the range 444-447 nm. This is the first time PL shoulders in the blue region are reported from pulsed laser ablated $SrAl_2O_4:Eu^{2+},Dy^{3+}$ thin films deposited at 400 ^oC temperature. Sato et al. [4] reported on the

blue PL peak from pulsed laser deposited $SrAl_2O_4:Eu^{2+},Dy^{3+}$ thin films at about 450 nm which featured only at lower temperatures (< 200 K). They attributed the peak to the other site of Sr^{2+} in the crystal host.

The deconvoluted Gaussian multiple peaks for the three different film spectra are shown in Figure 5. The deconvoluted peaks positions didn't go beyond the wavelength of 597 nm and the peak positions for films deposited at lower fluencies were similar (447, 530, 567 nm and 447, 525, 574 nm for the film deposited at laser fluencies 1.03 and 1.27 J/cm^2 respectively). They differed slightly from the film deposited at the highest laser fluence (447, 444, 538, 619 nm).

Figure 6 shows the long afterglow (phosphorescence) characteristics of the thin films deposited at different laser fluencies. Consistent with the PL data in Figure 4 and 5, the film prepared at laser fluence of 1.27 J/cm^2 has the highest initial intensity followed by the film deposited at the laser fluence of 1.78 J/cm^2.

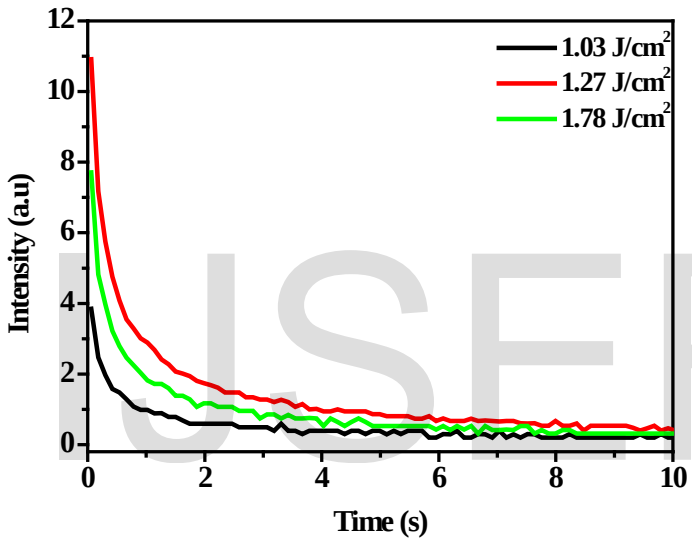

Fig. 6. The afterglow curves for PLD $SrAl_2O_4:Eu^{2+}$, Dy^{3+} thin films deposited at different laser fluencies.

It is evident from the results that better PL and afterglow properties are coming from the films with well-defined grains AFM images, consistent with the previously published results [5, 7]. However, one would expect the film deposited at the highest laser fluence to give the brightest emission, since it is the thickest as observed in the depth profile results in section 3.6 of this work and thicker films (deposited at higher number of pulses) tend to have superior PL properties [5]. A possible explanation to this trend is that the previous investigation holds only at lower fluencies (0.74 J/cm^2). It is reasonable to conclude that a combination of higher laser fluence and larger number of laser pulses (25,000 this work) is not desirable for high PL intensity desirable for high PL intensity of laser ablated $SrAl_2O_4:Eu^{2+},Dy^{3+}$ thin films.

3.5 The XPS results

Figure 7 shows the XPS spectra of the $SrAl_2O_4:Eu^{2+},Dy^{3+}$ thin films deposited at different laser fluencies. The survey spectra for films deposited at different laser fluencies (Fig 7 (a)) display similar peaks, coming from O, Sr, C and Al. The comparisons of

Al2p, Sr3d and O1s spectra are shown in Figure 7 (b)-(d). A similar pattern is observed in all spectra with the exception of some small shifts from the sample deposited at 1.27 J/cm² in the Al2p and Sr3d spectra.

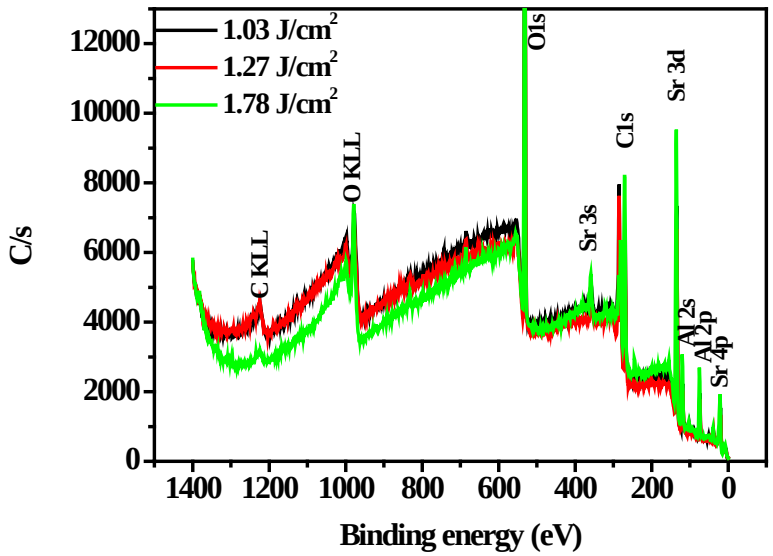

(a)

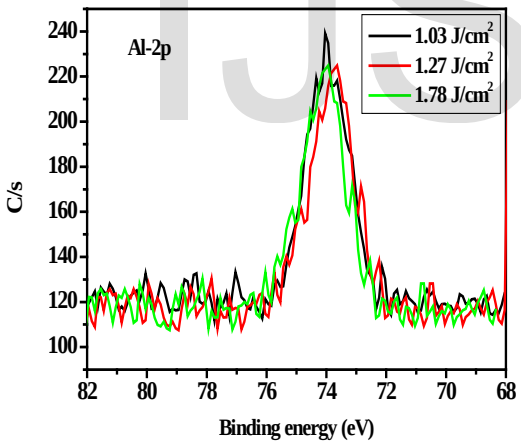

(b)

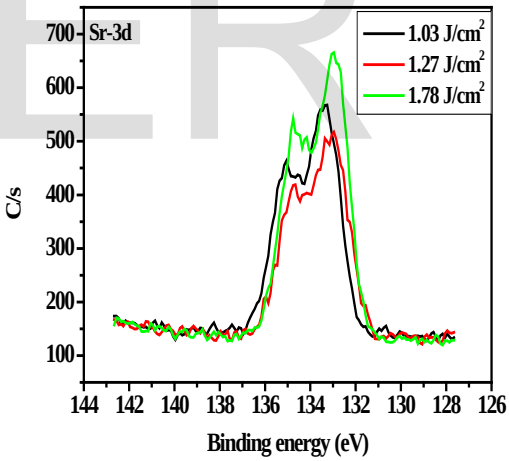

(c)

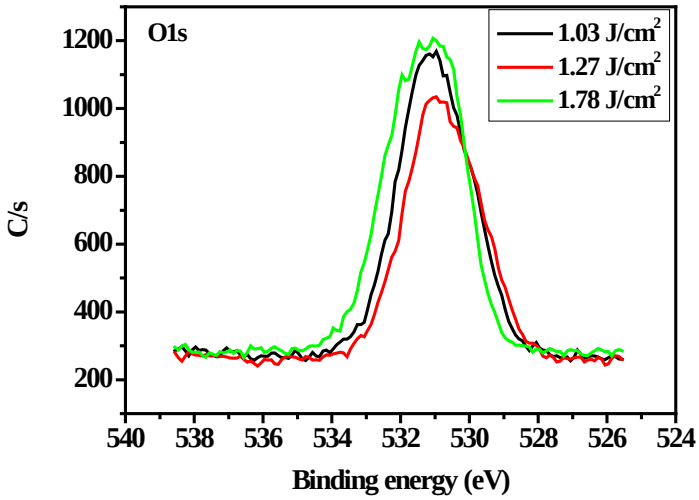

(d)

Fig. 7. (a) The XPS survey spectra for $SrAl_2O_4:Eu^{2+},Dy^{3+}$ thin films (b)-(d) are the comparisons of Al2p, Sr3d and O1s spectra for films deposited at different laser fluencies.

The XPS fittings for the three oxidation states Al2p, Sr3d and O1s of $SrAl_2O_4:Eu^{2+},Dy^{3+}$ thin films were also similar for all the films in this work. Figure 8 shows the fittings for film deposited at 1.78 J/cm². There are two peaks on the Al2p region (Figure 8 (a)) one at 74.02 eV from $SrAl_2O_4$ and another at 74.05 eV from Al_2O_3. These peak positions are relatively lower than those reported in our previous results [10] where the peak positions for the two materials were at 74.3 eV and 74.8 eV for $SrAl_2O_4$ and Al_2O_3 respectively. In the case of Sr3d region, (Figure 4(B) (b)) there are four peaks in total; Two peaks at 132.6 eV and 134.8 eV from Sr-$3d_{3/2}$ compared with 134.9 eV and 135.8 eV [10]. Two other peaks at 132.8 eV and 134.9 eV from Sr-$3d_{5/2}$ compared with 133.2 eV and 134.3 eV [10]. The two crystallographic positions of Sr^{2+} positions give rise to the two oxidation states, Sr-$3d_{3/2}$ and Sr-$3d_{5/2}$. On the O1s region, (Figure 8 (c)) two peaks are recorded at 530.4 eV, from $SrAl_2O_4$ and another peak at 531.7 eV from Al_2O_3. These two peak positions compare well with those reported in the literature, i.e. 530.6 [10] and 531.8 eV [12] for $SrAl_2O_4$ and Al_2O_3 respectively.

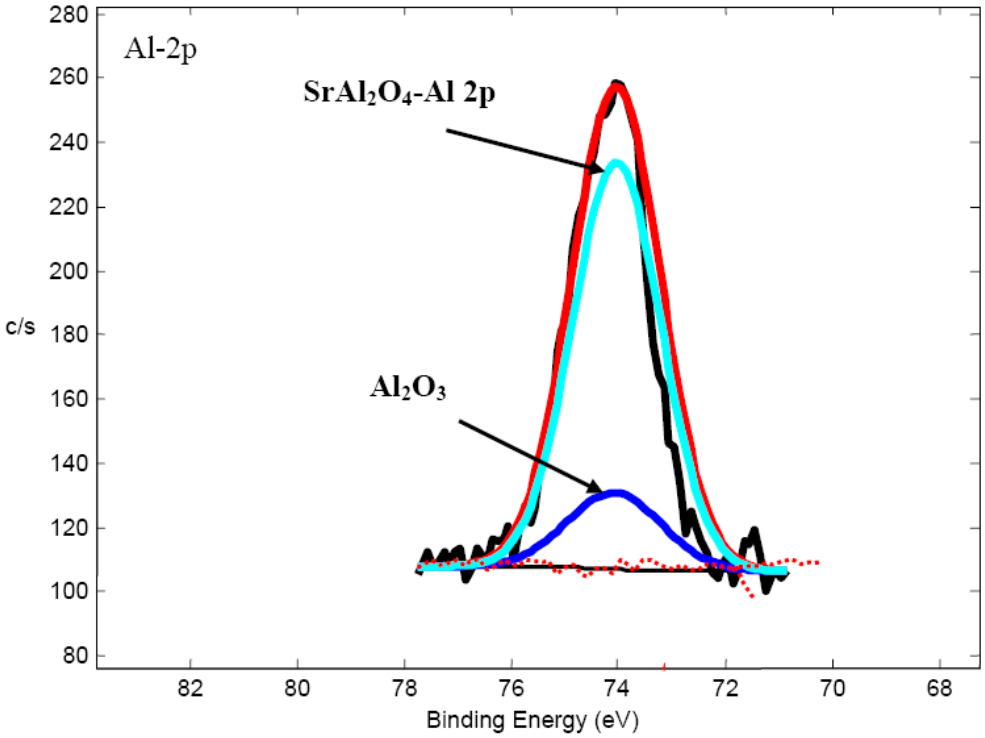
Al-2p
SrAl2O4-Al 2p
Al2O3
c/s
Binding Energy (eV)

(a)

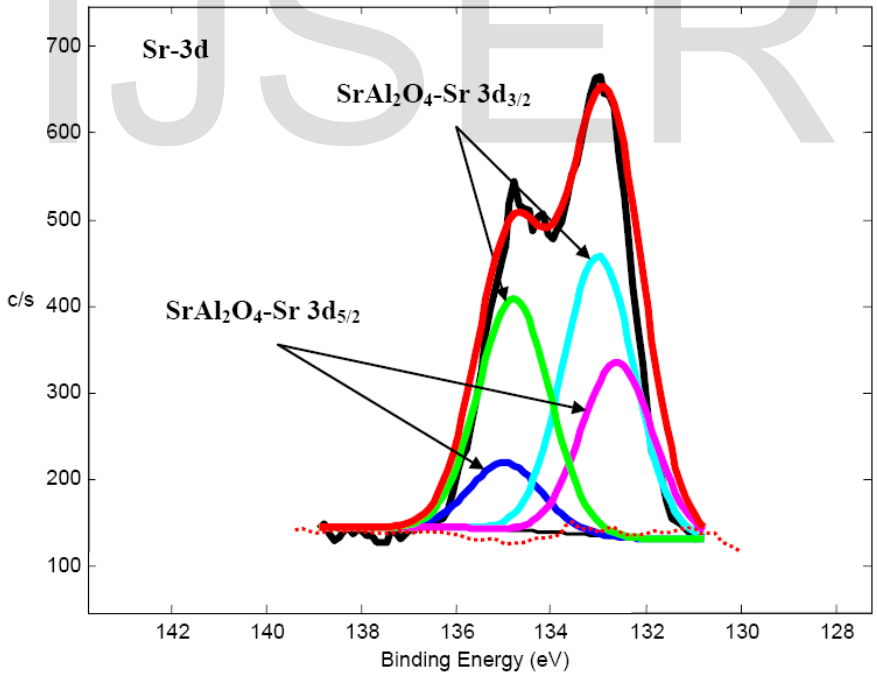
Sr-3d
SrAl2O4-Sr 3d3/2
SrAl2O4-Sr 3d5/2
c/s
Binding Energy (eV)

(b)

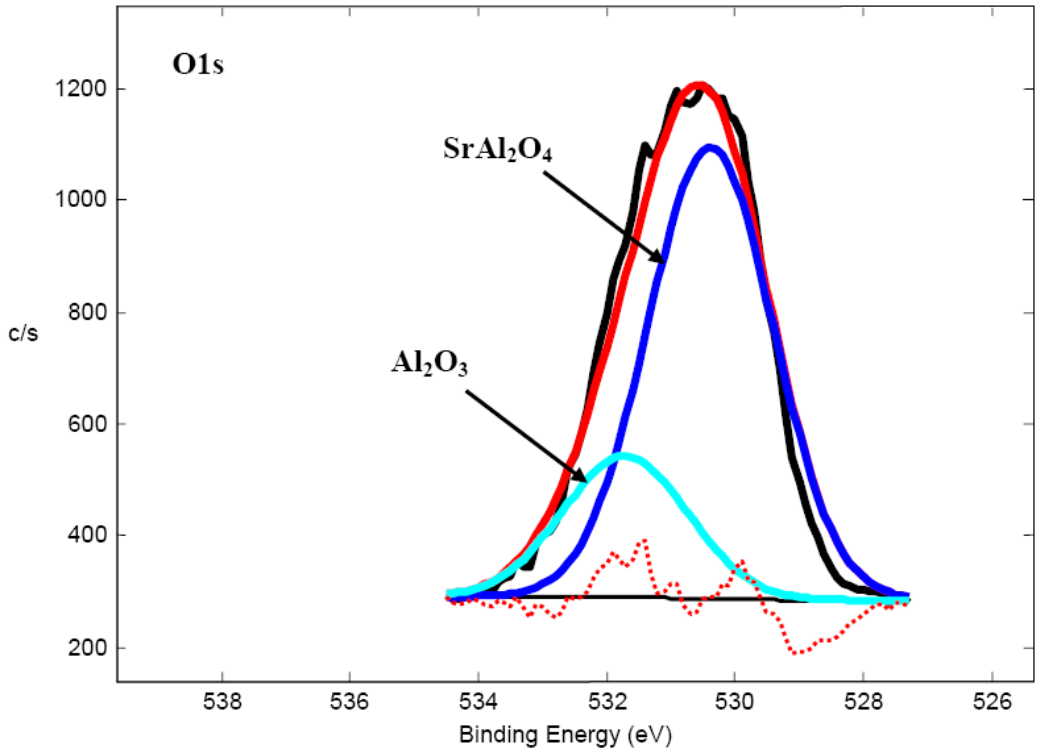

(c)

Fig. 8. The XPS fittings for (a) Al2p, (b) Sr3d and (c) O1s oxidation states for $SrAl_2O_4:Eu^{2+},Dy^{3+}$ films deposited at 1.78 J/cm² fluence.

3.6 The XPS depth profile results

Figure 9 shows the XPS survey spectra for the depth profiled films of a film deposited at 1.27 J/m2 at the beginning (Figure 9 (a)) of depth profiling and after 78 seconds (Figure 9(b). The survey spectrum at the beginning is mainly characterized by the binding energies of O, Sr and Al. However, after 78 seconds, the substrate seems to have been reached as can be substantiated by the emergence of Si2p from the substrate. There is also a Sr2s peak and Al2p traces.

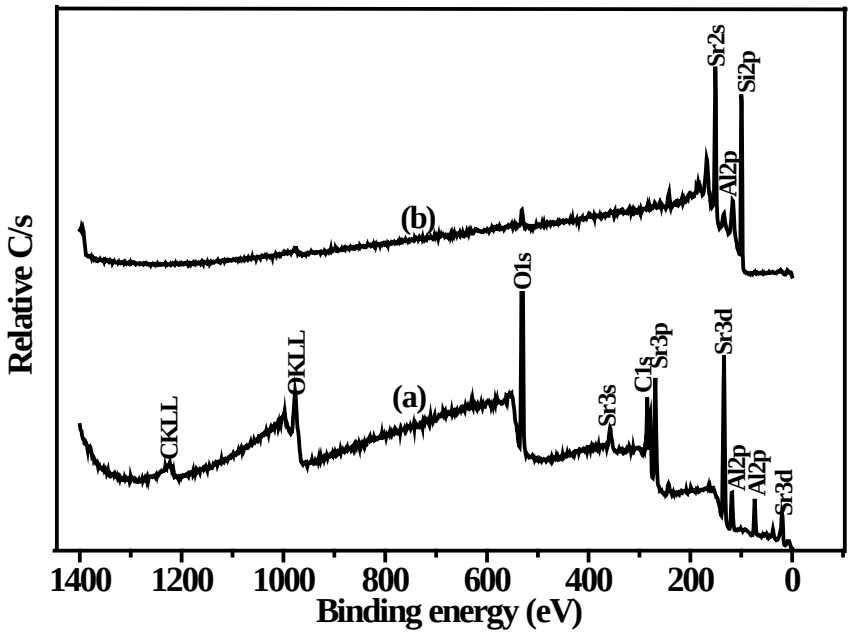

Fig. 9. The XPS depth profile spectra of $SrAl_2O_4:Eu^{2+},Dy^{3+}$ thin films deposited at laser fluence of 1.27 J/cm² at t = 0 minute and t = 78 minutes in Argon atmosphere.

The XPS depth profile in atomic concentration for the $SrAl_2O_4:Eu^{2+},Dy^{3+}$ thin films are represented by Figure 10 (a), 10 (b) and 10 (c) for films deposited at laser fluencies of 1.03 J/cm², 1.27 J/cm² and 1.78 J/cm² respectively. All depth profiles are characterized by the main elements of $SrAl_2O_4:Eu^{2+},Dy^{3+}$ material, i.e. Sr, Al, and O. The C was coming from the atmospheric contamination while Si was coming from the substrate. The films show a good distribution of elemental compositions across the entire film thickness. In all the depth profiles, the concentration of O was the highest followed by Al and then Sr. The concentrations of C and Si were at the values close to zero across the film layer. In our previous results [10], Sr element had higher elemental percentage compositions in the $SrAl_2O_4:Eu^{2+},Dy^{3+}$ than Al. The higher number of pulses (25000) and higher temperature (400 °C) compared to the previous results (8000 pulses) and 200 °C are possibly the contributing factor to the layers arrangements.

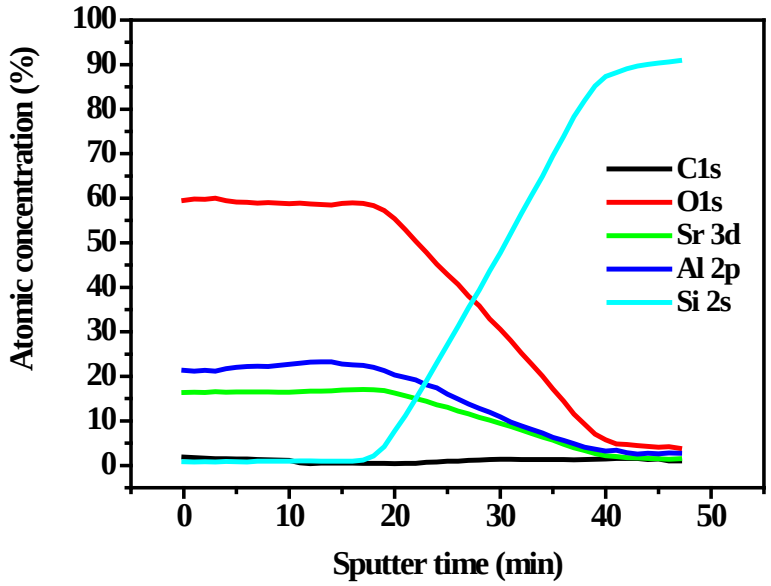
Atomic concentration (%)
Sputter time (min)
C1s
O1s
Sr 3d
Al 2p
Si 2s

(a)

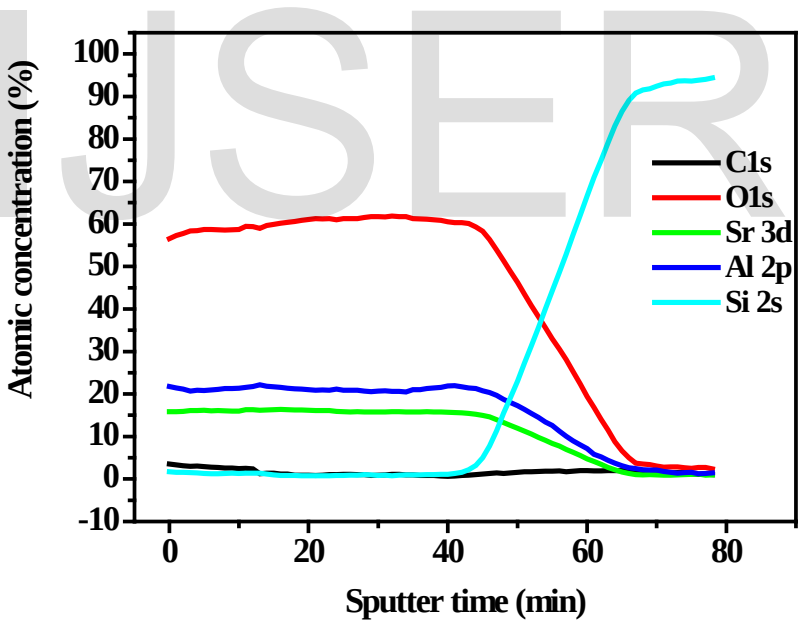
Atomic concentration (%)
Sputter time (min)
C1s
O1s
Sr 3d
Al 2p
Si 2s

(b)

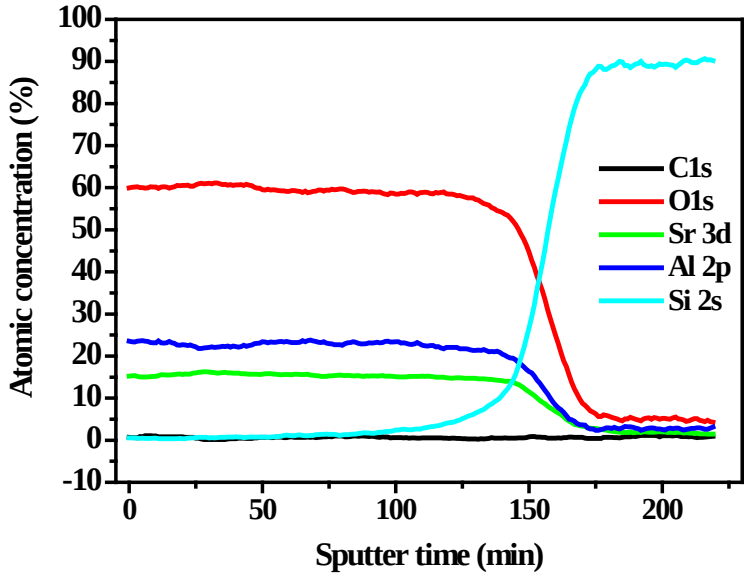

(c)

Fig. 10. The XPS depth profile spectra of $SrAl_2O_4:Eu^{2+},Dy^{3+}$ thin films deposited at laser fluencies (a) 1.03 J/cm² (b) 1.27 J/cm² and (c) 1.78 J/cm².

Another observation which slightly differs from our previous [5] results , is that C was decreasing with sputter time before attaining the lowest value, but this time its variation is constant throughout the sputtering process. This suggests that the films from the current work were less contaminated by the atmosphere compared to those of our previous work. The Ar ion gun sputter rate was the same (8.5 nm/min) for all the films, the time taken to sputter the films deposited at 1.03 J/cm², 1.27 J/cm² and 1.78 J/cm² laser fluencies were 48 min, 78 min and 220 min respectively. Their respective thicknesses were 408nm, 663 nm, and 1870 nm. Thicker films were obtained from higher laser fluencies because the thickness depends on the laser fluence [9]. It can also be noted that the approximate average atomic percentage Sr/Al ratio for the thin films decreased from 0.76 to 0.63 for the films deposited at the laser fluencies of 1.03 J/cm² and 1.78 J/cm² respectively.

4. Conclusion

Long afterglow $SrAl_2O_4:Eu^{2+},Dy^{3+}$ thin film phosphors were successfully deposited on Si substrates by pulsed laser deposition technique. The laser fluence has proved to be a key deposition parameter in the preparations of $SrAl_2O_4:Eu^{2+},Dy^{3+}$ thin films. $SrAl_2O_4:Eu^{2+},Dy^{3+}$ thin films gave two green emission peaks coming from two sites of Sr^{2+} in the crystal host. Well-defined nano-grains were found to be accompanied by superior PL intensity and afterglow properties. The film with optimum PL properties was obtained from the intermediate laser fluence (1.27 J/cm²) and the upper/lower values gave lower PL and afterglow intensities. The green emission peaks were attributed to the $4f^65d^1 \rightarrow 4f^7$ transitions of Eu^{2+} ions. The as-deposited films were all amorphous. The EDS and XPS spectra contained all the main elements of the host material, i.e. Sr, Al, and O plus the adventitious C. The depth profile analysis showed a uniform distribution of atomic elemental composition across the film.

Acknowledgement

The African Laser Centre (ALC), National Research Fund (NRF) and the Nano materials cluster program of the University of the Free State are acknowledged for their financial support.

References

1. Harish Chander, D. Haranath, Virendra Shanker, Pooja Sharma, "Synthesis of nanocrystals of long persisting phosphor by modified combustion technique", *J. Cryst. Growth,* **271,** pp 307-312, Oct. 2004 (Journal citation).

2. Kyoung Bo Han, Chang Hoon Jeon, Hee Sauk Jhon, Sang Yeol Lee, "Effect of laser fluence on the ferroelectric properties of pulsed laser deposited $(Pb_{1-x}La_x)Ti_{1-x/4}O_3$ thin films" *Thin Solid Films* **437,** pp 285-289, Aug. 2003 (Journal citation).

3. M.O. Ntwaeaborwa, P.D. Nsimama, E. Coetsee, J. H.C. Swart, "The effects of substrate temperature on the structure, morphology and photoluminescence properties of pulsed laser deposited $SrAl_2O_4:Eu^{2+},Dy^{3+}$ thin films" *Physica B: Condensed Matter*, **404**, pp 4436-4439, Mar. 2009 (Conference proceedings).

4. K. Sato et al. K. Sato, S. Komuro, T. Morikawa, H. Aizawa, T. Katsumata, S. Harako, X. Zhao, "Long afterglow characteristics of thin film phosphor fabricated by laser ablation" *J. of Cryst. Growth* **275,** pp e1137–e1141, Feb. 2005 (Conference proceedings)

5. P.D. Nsimama, M.O. Ntwaeaborwa, E. Coetsee, H.C. Swart, "The influence of the number of pulses on the morphological and photoluminescence properties of $SrAl_2O_4:Eu^{2+},Dy^{3+}$ thin films prepared by pulsed laser deposition" *Physica B: Condensed Matter*, **404**, pp 4489-4492, Mar. 2009 (Conference proceedings).

6. M.O. Ntwaeaborwa, P.D. Nsimama, S. Pitale, I. M. Nagpure, V. Kumar, E. Coetsee, J. J. Terblans, P. T. Sechogela and H. C. Swart, "Photoluminescence properties of thin phosphor films grown by pulsed laser deposition" *J. Vac. Sci. Tech. A* **28,** pp 901-905, Jul. 2010 (Conference proceedings).

7. P.D. Nsimama, M.O. Ntwaeaborwa, H.C. Swart, "The effect of different gas atmospheres on luminescent properties of pulsed laser ablated $SrAl_2O_4:Eu^{2+},Dy^{3+}$ thin films" *Journal of Lum.* **131**, pp (2011) 119-125, Jan. 2011 (Journal citation).

8. R. Eason (ed.) *Pulsed laser deposition of thin films: Applications-led growth of functional materials*, Hoboken, USA, Wiley Interscience, pp 3- 28, 2006 (Book style).

9. H. ElGazzar, E. Abdel-Rahman, H.G. Salem, F. Nassar, "Preparation and characterizations of amorphous nanostructured SiC thin films by low energy pulsed laser deposition" *Appl. Surf. Sci*. **256**, pp 2056-2060, Jan. 2010 (Journal citation).

10. P.D. Nsimama, M.O. Ntwaeaborwa, H.C. Swart, "Auger electron/X-ray photoelectron and cathodoluminescent spectroscopic studies of pulsed laser ablated $SrAl_2O_4:Eu^{2+}Dy^{3+}$ thin films" *Appl. Surf. Sci.* **257,** pp 512-517, Nov. 2010 (Journal citation).

11. F. Clabau, X. Rocquefelte, S. Jobic, P. Deniard, M.-H. Whangbo, A. Garcia, T. Le Mercier, "Mechanism of Phosphorescence Appropriate for the Long-Lasting Phosphors Eu^{2+}-Doped $SrAl_2O_4$ with Codopants Dy^{3+} and B^{3+}, *Chem. Mater*. **17** pp 3904-3912, Jul. 2005 (Journal citation).

12. C.D. Wagner, D.E. Passoja, H Taylor, F. Hillery, T.G. Kinisky, H.A. Six, W.T. Jansen, J.A, "Auger and photoelectron line energy relationships in aluminum–oxygen and silicon–oxygen compounds" *J. Vac. Sci. Technol.* **21**, pp 933-944, Nov. 1982 (Journal citation).